Advanced Summer School on
"Laser-Driven Sources of High Energy Particles and Radiation"
9-16 July 2017, Capri, Italy

Consiglio Nazionale
delle Ricerche

INO-CNR
ISTITUTO
NAZIONALE DI
OTTICA

Istituto Nazionale di
Fisica Nucleare

Ultrafast, intense laser pulse diagnostics
(Lecture 2 of 2)

Luca Labate

Istituto Nazionale di Ottica
Consiglio Nazionale delle Ricerche
Pisa, Italy

Also at
Istituto Nazionale di Fisica Nucleare
Sezione di Pisa, Italy

Outline

Lecture 1 of 2

A (not so short) introduction to the mathematical description of the temporal behaviour of ultrashort laser pulses (terminology,, basic facts, ...)

- Spectral amplitude and phase
- Dispersion, dispersion compensation

Experimental techniques for the temporal characterization of ultrashort laser pulses

- Photodiodes, streak camera
- 1st and 2nd order autocorrelators

Lecture 2 of 2

- Advanced techniques for the pulse length and spectral phase measurements: FROG, SPIDER
- Contrast measurement techniques (in brief)

Transverse functions characterization and wavefront correction

- Wavefront characterization techniques
- Wavefront correction and beam focusing

Characterization of the temporal behaviour of a laser pulse w/o a reference pulse
1st order autocorrelation

Let's look at what happens when we have an interferometric *auto*-correlator: that is the pulse to be measured is splitted into two arms and recombined after being relatively time-delayed

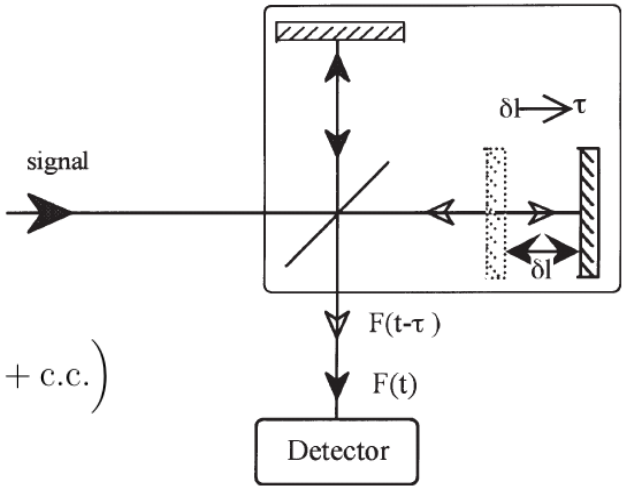

$$
\begin{aligned}
S(\tau) &\propto \int_{-\infty}^{+\infty} |E(t-\tau)+E(t)|^2 \, \mathrm{d}t \\
&= \int_{-\infty}^{+\infty} |E(t-\tau)|^2 \, \mathrm{d}t + \int_{-\infty}^{+\infty} |E(t)|^2 \, \mathrm{d}t + \left(\int_{-\infty}^{+\infty} E(t)E^*(t-\tau) \, \mathrm{d}t + \mathrm{c.c.} \right) \\
&= 2\int_{-\infty}^{+\infty} |E(t)|^2 + \left(\int_{-\infty}^{+\infty} E(t)E^*(t-\tau) \, \mathrm{d}t + \mathrm{c.c.} \right)
\end{aligned}
$$

The terms in parenthesis correspond to the 1st order **auto**-correlation function.

Wiener-Khinchin theorem* $\mathcal{F}[G_1(\tau)] = \left|\tilde{E}(\omega)\right|^2$

Thus, taking the FT of the signal (with respect to the time delay between the two pulses), one ultimately only gets the power spectrum (Fourier-transform spectroscopy): no infos on the spectral phase

In fact, it can be shown that the full knowledge of $E(t)$ requires the measurement of all the successive $G_n(t)$

*see for instance Born, Wolf, *Principles of Optics*

Characterization of the temporal behaviour of a laser pulse w/o a reference pulse
1st order autocorrelation

Recalling that $E(t) = A(t)\mathrm{e}^{i\Phi_0}\mathrm{e}^{i\omega_0 t}\mathrm{e}^{i\Phi_a(t)}$

$$\begin{aligned} S(\tau) &\propto 2\int_{-\infty}^{+\infty} |E(t)|^2 + \left(\int_{-\infty}^{+\infty} E(t)E^*(t-\tau)\,\mathrm{d}t + \mathrm{c.c.}\right) \\ &= 2\int_{-\infty}^{+\infty} |E(t)|^2\,\mathrm{d}t + 2\int_{-\infty}^{+\infty} A(t)A(t-\tau)\cos\left[\omega_0\tau + \Phi_a(t) - \Phi_a(t-\tau)\right]\mathrm{d}t \\ &\propto 1 + G_1(\tau) \end{aligned}$$

Unchirped pulse

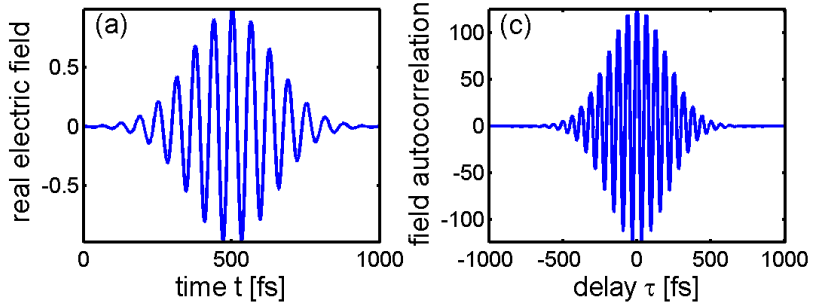

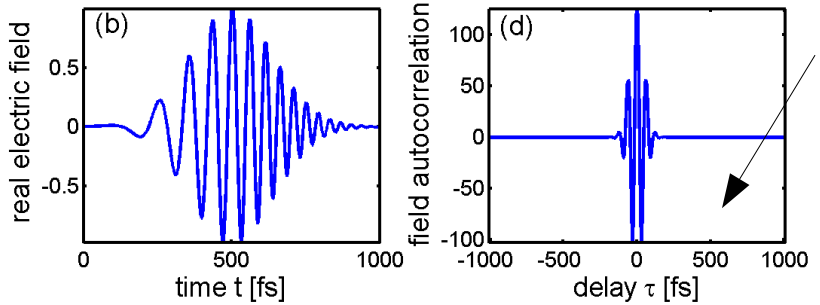

Chirped pulse

The trace is symmetric, even in the presence of a chirp

Using only a Michelson interferometer: the width of S(t) is related to the coherence length of the pulse.

No way to recover the phase: 1st order autocorrelation is the IFT of the spectrum

Quite difficult to interpret, w/o any hint on the pulse chirp, spectrum, ...

With some assumption on both the pulse shape and phase (basically, no or negligible chirp), one can recover the pulse duration

Very basic method!

Characterization of the temporal behaviour of a laser pulse w/o a reference pulse: 2nd order autocorrelation

We now insert a 2nd harmonic crystal (and a filter) before the detector

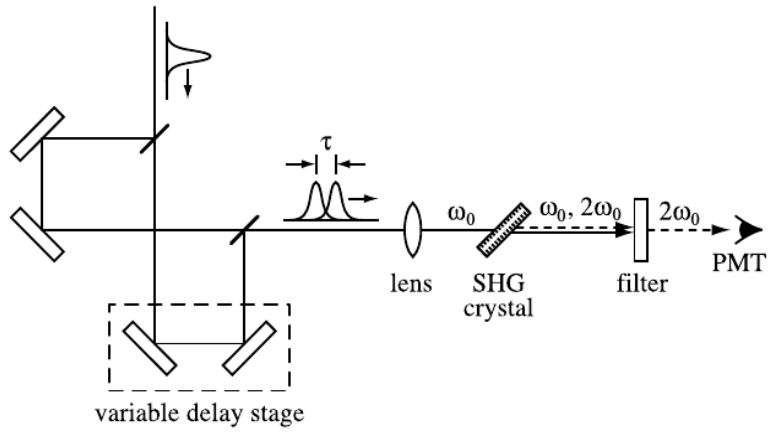

Remember that

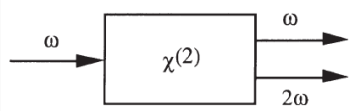

$$P_i(2\omega) = \sum_{j,k} \chi^{(2)}_{ijk} E_j(\omega) E_k(\omega)$$

$$P(2\omega) \propto (E(t) + E(t-\tau))(E(t) + E(t-\tau))$$

$$E_{2\omega} \propto (E(t) + E(t-\tau))(E(t) + E(t-\tau))$$

The observed signal is thus

$$E(t) = A(t)e^{i\Phi_0}e^{i\omega_0 t}e^{i\Phi_a(t)}$$

$$\begin{aligned} S(\tau) &\propto \int_{-\infty}^{+\infty} \left|(E(t) + E(t-\tau))^2\right|^2 \, \mathrm{d}t \\ &= \int_{-\infty}^{+\infty} \left|\left(A(t)e^{i\omega_o t}e^{i\Phi_a(t)} + A(t-\tau)e^{i\omega_0(t-\tau)}e^{i\Phi_a(t-\tau)}\right)^2\right|^2 \, \mathrm{d}t \\ &\vdots \\ &= \int_{-\infty}^{+\infty} \mathrm{d}t \Big[A^4(t) + A^4(t-\tau) + 4A^2(t)A^2(t-\tau) + \\ &\quad + 4A(t)A(t-\tau)\left(A^2(t) + A^2(t-\tau)\right)\cos\left(\omega_0\tau + \Phi_a(t) - \Phi_a(t-\tau)\right) \\ &\quad + 2A^2(t)A^2(t-\tau)\cos\left(2(\omega_0\tau + \Phi_a(t) - \Phi_a(t-\tau))\right)\Big] \end{aligned}$$

Characterization of the temporal behaviour of a laser pulse w/o a reference pulse: 2nd order interferometric autocorrelation

$$S(\tau) \propto I_{background} + I_{IA}(\tau) + I_{\omega_0}(\tau) + I_{2\omega_0}(\tau)$$

$$\begin{aligned}
I_{background} &= \int_{-\infty}^{+\infty} A^4(t)\,\mathrm{d}t + \int_{-\infty}^{+\infty} A^4(t-\tau)\,\mathrm{d}t = 2\int_{-\infty}^{+\infty} I^2(t)\,\mathrm{d}t \\
I_{IA}(\tau) &= 4\int_{-\infty}^{+\infty} A^2(t)A^2(t-\tau)\,\mathrm{d}t = 4\int_{-\infty}^{+\infty} I(t)I(t-\tau)\,\mathrm{d}t \\
I_{\omega_0}(\tau) &= 4\int_{-\infty}^{+\infty} A(t)A(t-\tau)(A^2(t)+A^2(t-\tau))\cos\left[\omega_0\tau + \Phi_a(t) - \Phi_a(t-\tau)\right]\,\mathrm{d}t \\
I_{2\omega_0}(\tau) &= 2\int_{-\infty}^{+\infty} A^2(t)A^2(t-\tau)\cos\left[2(\omega_0\tau + \Phi_a(t) - \Phi_a(t-\tau))\right]\,\mathrm{d}t
\end{aligned}$$

Fringes at the carrier frequency (modified by higher order terms) appear in the measured trace due to the interference among the different SH signals

Contrast: 8 to 1
(this is independent of any experimental arrangement)

$$S(\tau = 0) \propto 16\int_{-\infty}^{+\infty} I^2(t)\,\mathrm{d}t$$

$$S(\tau \to \infty) \propto \int_{-\infty}^{+\infty} I^2(t)\,\mathrm{d}t$$

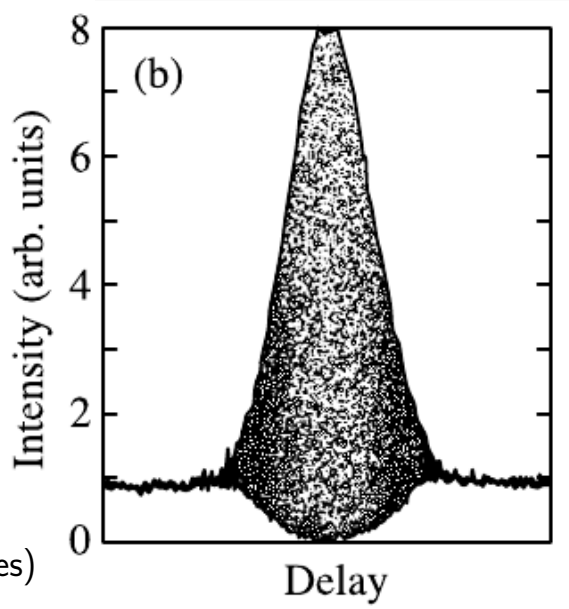

The shape of the fringe envelope is very sensitive to the pulse amplitude but, which is more important, depends on the instantaneous frequency of the laser pulse
(Time slices of the pulse having very different frequencies do not give clear fringes)
Notice, however, that the contrast remains in any case unaffected! This can be used as a way to check the autocorrelator alignment

Characterization of the temporal behaviour of a laser pulse w/o a reference pulse: 2nd order interferometric autocorrelation

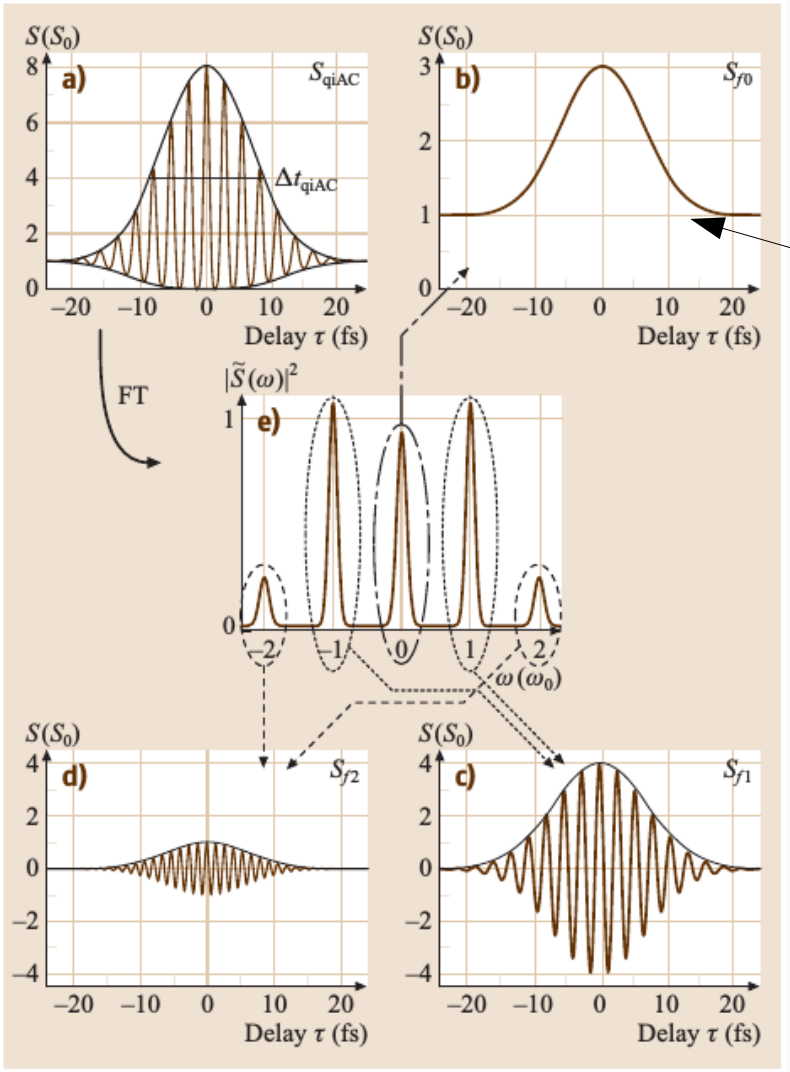

This corresponds to averaging over the oscillations.
This is called "non bakground free Intensity Autocorrelation"
A similar condition can be obtained avoiding the interference terms with a slightly modified setup

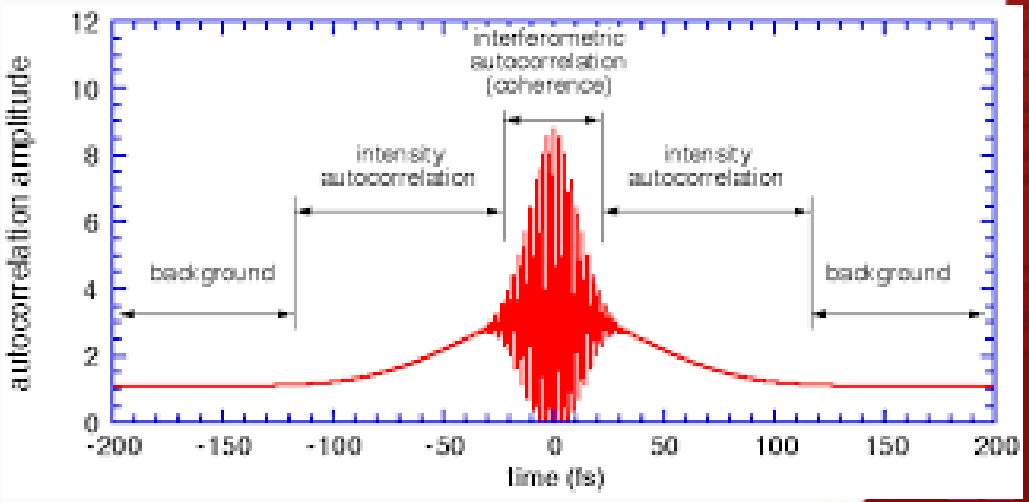

Background-free 2nd order Intensity Autocorrelation

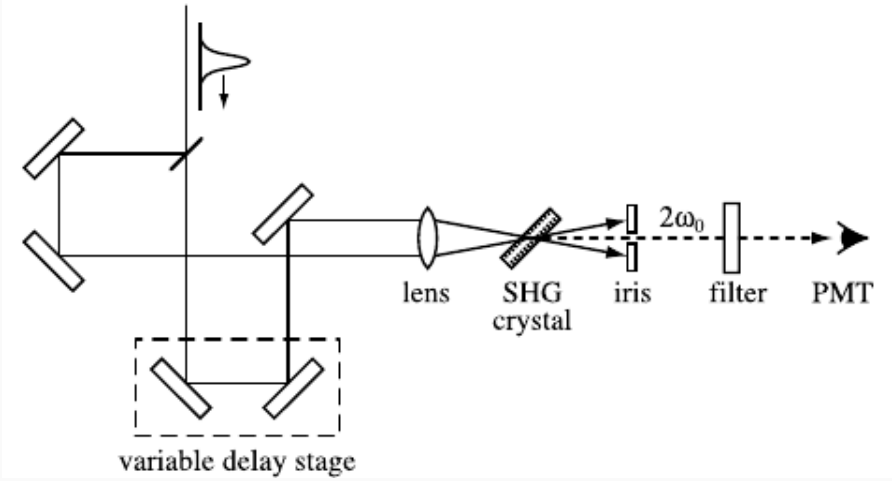

It is easy to demonstrate that in this case the signal is just proportional to the second order autocorrelation (that is, with respect to the above case, no background and no interference terms are observed)

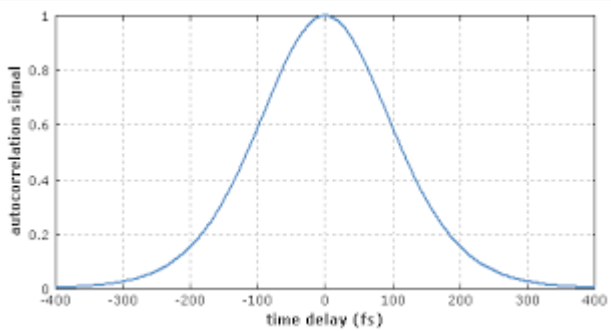

The pulses exhibit no overlap for delays much greater than the pulse width, when the (2nd order) correlation function goes to zero. The width of the correlation peak gives information about the pulse width

The (2nd order) correlation function is an even function of τ, independent of the simmetry of the actual pulse. Therefore, one cannot uniquely recover the pulse intensity profile

If one knew a priori that the intensity profile were symmetric, one could recover *I(t)*. Indeed

$$\mathcal{F}[G_2(\tau)] \propto \left|\tilde{I}(\omega)\right|^2 \qquad \text{where} \qquad \tilde{I}(\omega) := \mathcal{F}[I(t)]$$

If *I(t)* is symmetric, then its FT is real and can be therefore recovered knowing its module only. Conversely, if *I(t)* is not symmetric, the phase of its FT would be needed to retrieve it

Background-free 2nd order Intensity Autocorrelation: single shot autocorrelator

The background-free (non collinear) autocorrelation can be actually used to build single-shot autocorrelators

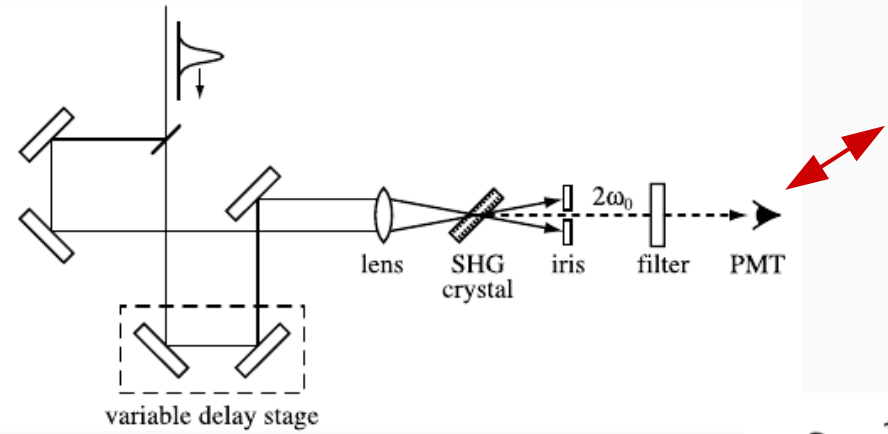

The delay t is now "encoded" into the spatial position x

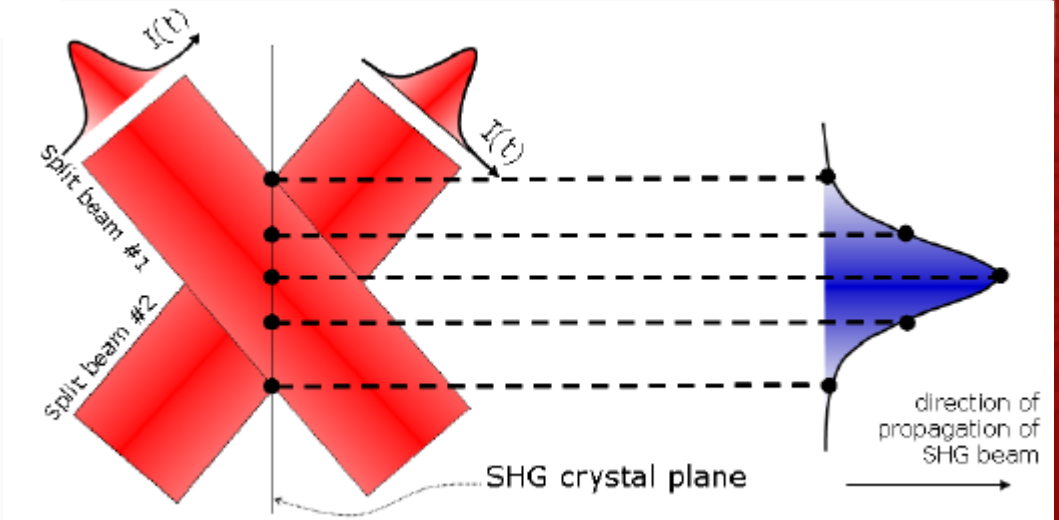

INO-CNR
ISTITUTO
NAZIONALE DI
OTTICA

Background-free 2nd order Intensity Autocorrelation: single shot autocorrelator

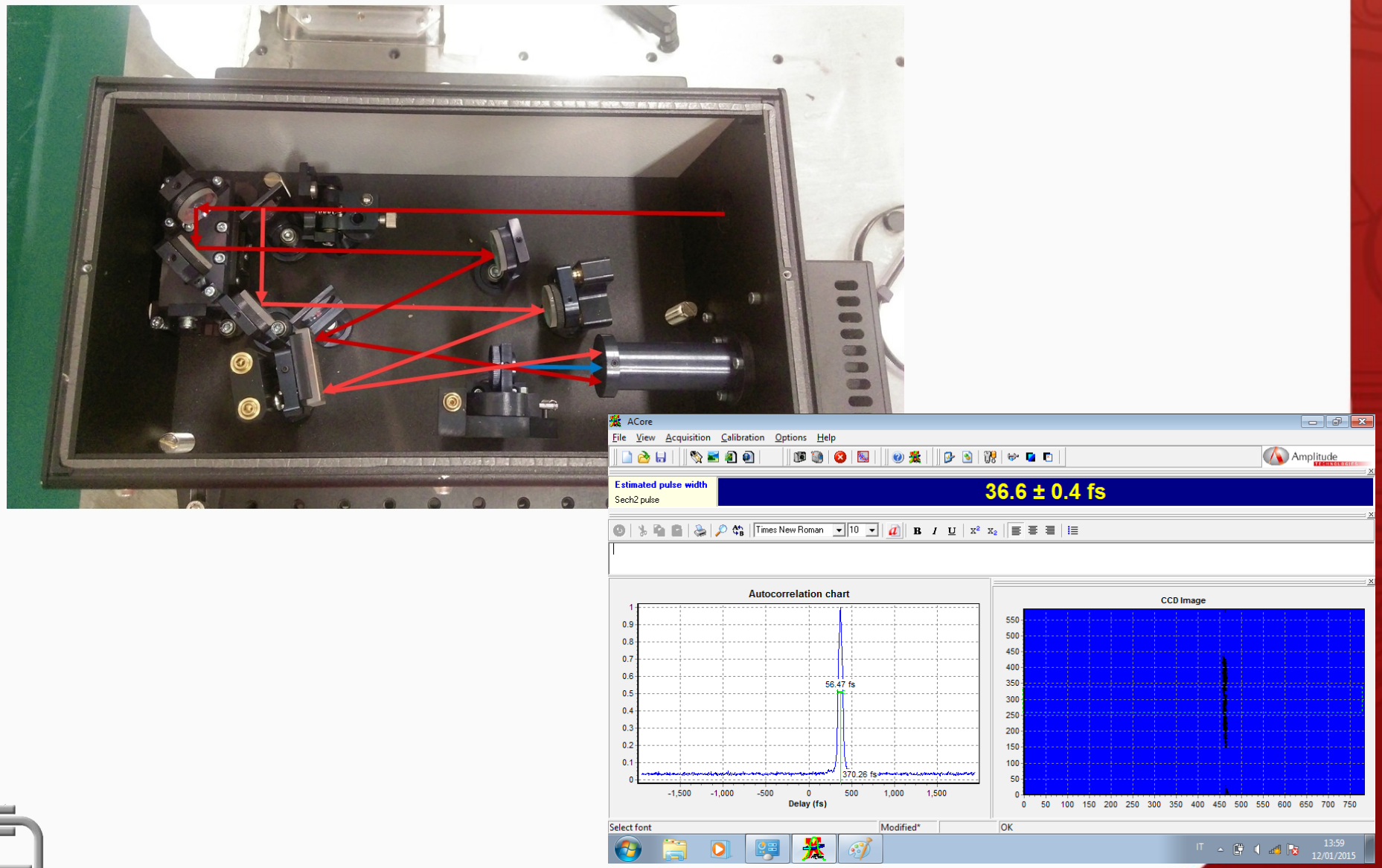

A few examples of signals observed with 2nd order Interferometric Autocorrelation

Let's go back to the Interferometric Autocorrelation
and see some examples of pulses with different chirps

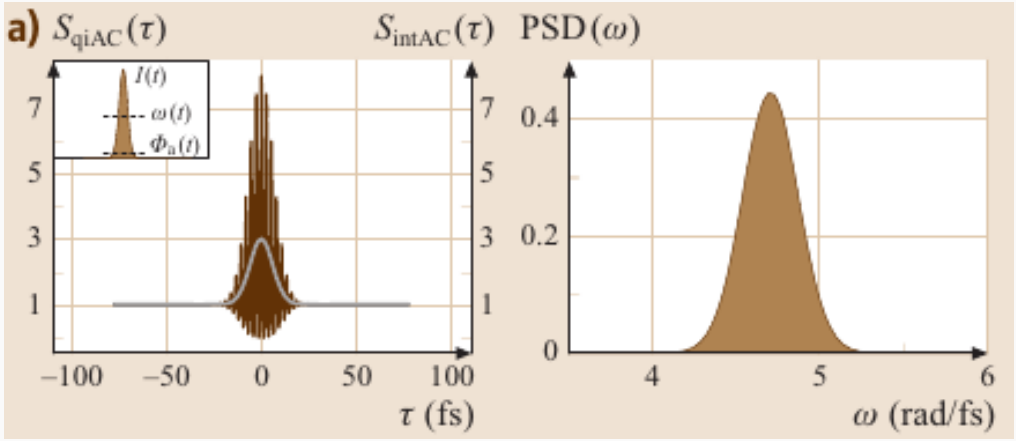

Unchirped pulse

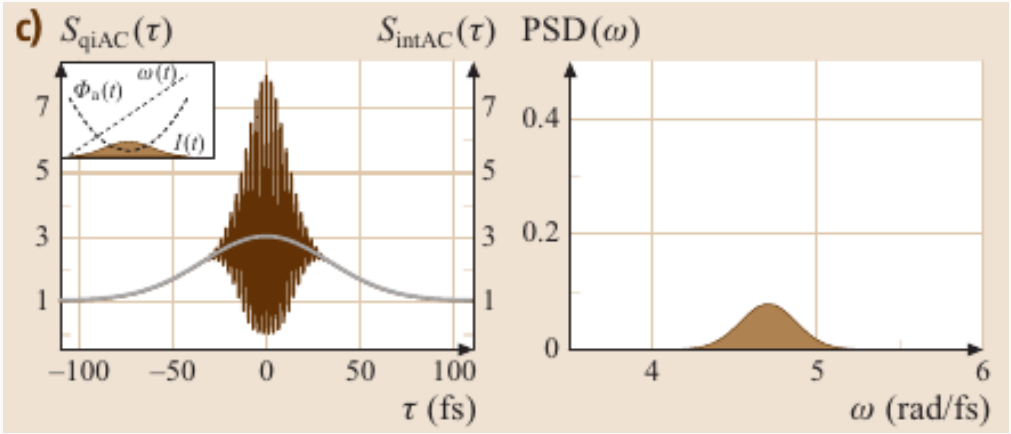

Symmetrically broadened pulse, due to a
2nd order spectral phase term

A few examples of signals observed with 2nd order Interferometric Autocorrelation

As it can be easily understood, the original pulse giving rise to a given Interferometric Autocorrelation trace is not unique

Asymmetric pulse

Symmetric pulse

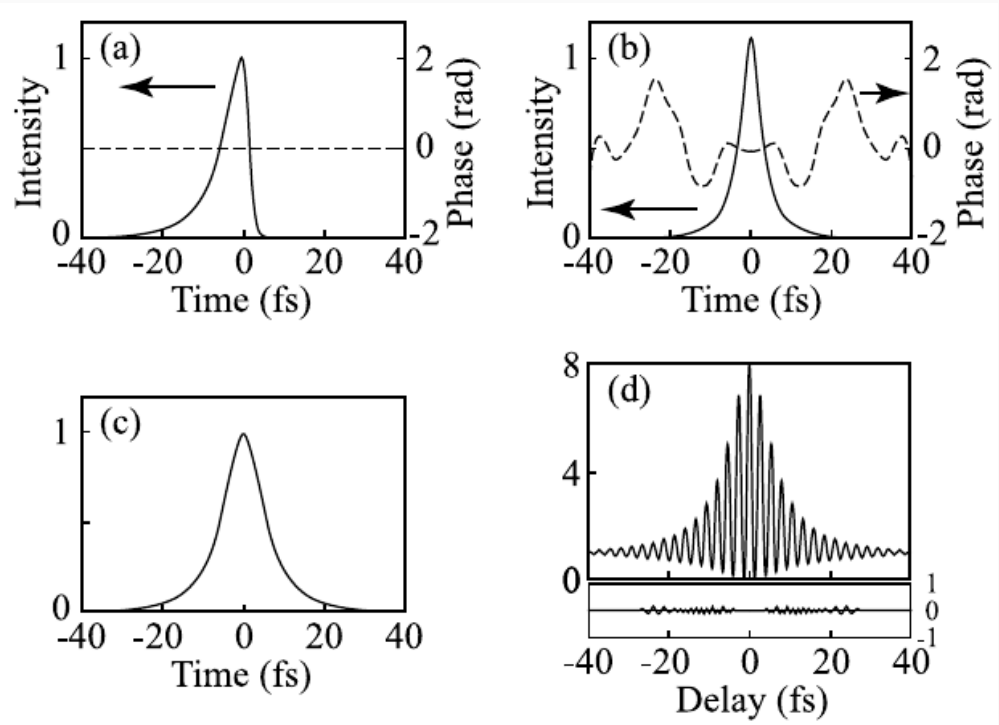

Intensity Autocorrelation

Interferometric Autocorrelation and difference between traces

(Limited) informations about the spectral phase can be obtained from Interferometric Autocorrelation using iterative algorithms

Most of the times, Interferometric Autocorrelation is used as a clear visual indicator of the pulse chirp

More advanced autocorrelation techniques are needed in order to retrieve the spectral phase

Pulse characterization: phase information?

To summarize on pulse measurement techniques so far:

Autocorrelation

Non-collinear (or Intensity Autocorrelation): no phase information
Collinear (Interferometric Autocorrelation): very limited phase informations

Pulse shape characterization techniques in the time-frequency domain

More advanced techniques involve both temporal resolution and spectral resolution at the same time, and they are able to provide both the pulse envelope (pulse duration) and the phase

One of the mostly used description of an ultrahort pulse in a time-frequency domain involves the use of so called "spectrograms"

How we can "measure" the instantaneous frequency of a pulse?

Electric field

Gate function, centered at τ

$$f_{signal}(t,\tau) = E(t)g(t-\tau)$$

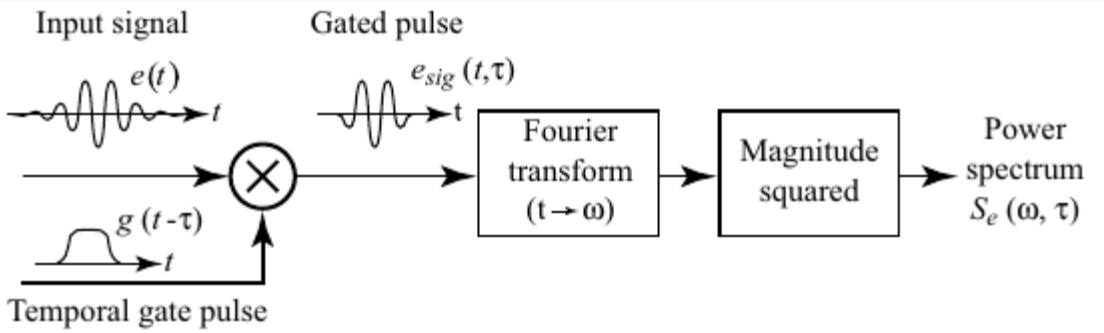

The spectrum of the field in a time interval around τ (whose width depends on the gate function) is then given by the square modulus of the FT (with respect to t) of this signal:

$$S(\omega,\tau) = \left|\mathcal{F}\left[f_{signal}(t,\tau)\right]\right|^2 = \left|\int_{-\infty}^{+\infty} E(t)g(t-\tau)\mathrm{e}^{-i\omega t}\,\mathrm{d}t\right|^2$$

An example of a spectrogram

Very complex pulse

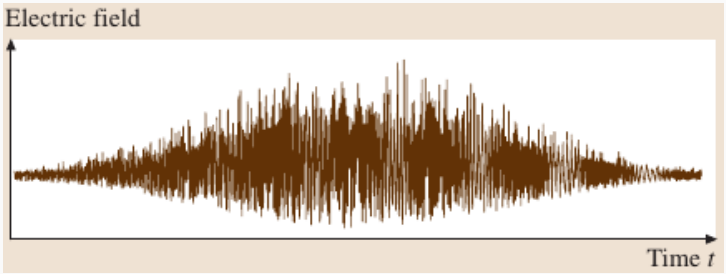

"Simple" pulses

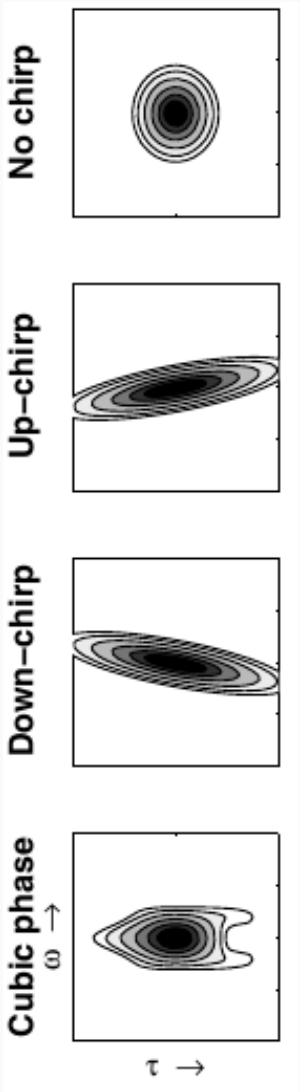

Measuring the spectrogram: the FROG technique

The main experimental challenge in measuring ultrafast optical spectrograms is in implementing an ultrafast gate function

In the FROG (Frequency Resolved Optical Gating) technique(s), the pulse is used to gate itself via a nonlinear optical interaction

Different FROG techniques have been developed, each employing different nonlinear effect

Different FROG implementation thus differ from each other for the gate function, that is the $f_{signal}(t,\tau)$ measured

$$f_{signal}(t,\tau) = E(t)g(t-\tau)$$

$$S(\omega,\tau) = \left| \int_{-\infty}^{+\infty} f_{signal}(t,\tau) \mathrm{e}^{-i\omega t}\, \mathrm{d}t \right|^2$$

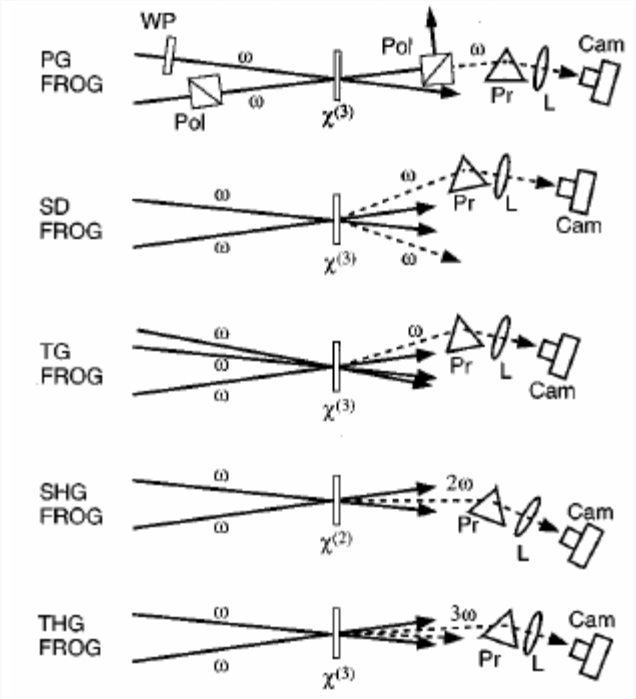

Polarization Gating FROG (PG FROG)

Ultrafast gating is achieved through the optical Kerr effect (3rd order nonlinearity)

The "gating pulse" induces birefringence and therefore a polarization rotation of the other pulse, which is thus transmitted through the 2nd polarizer

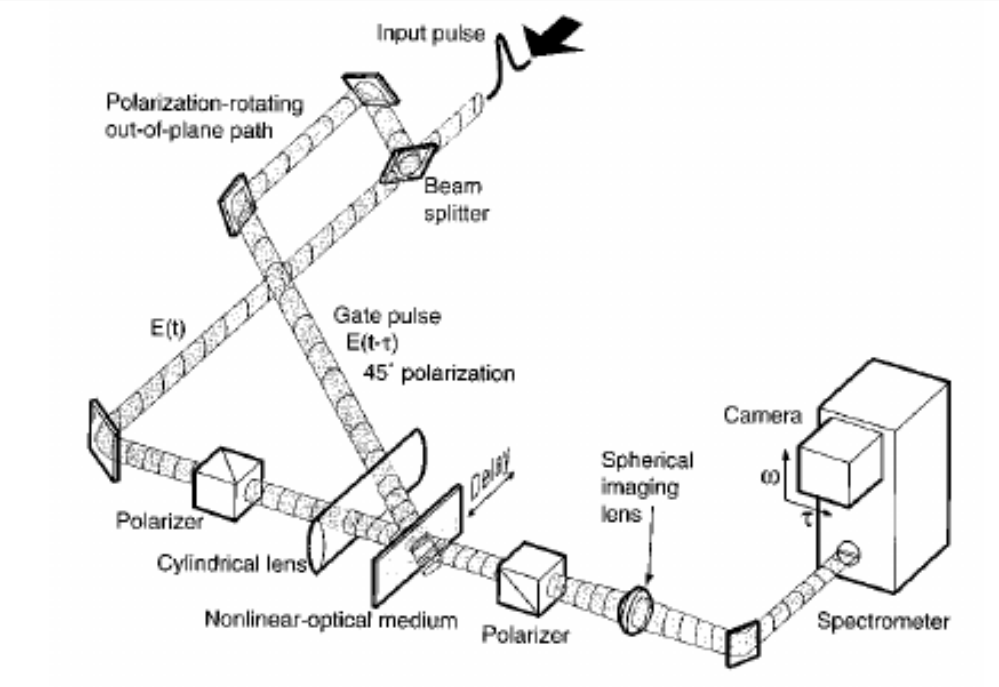

It is easy to check that in this case the gate is

$$g(t-\tau) = |E(t-\tau)|^2$$

and thus the signal

$$f_{signal}(t,\tau) = E(t)\,|E(t-\tau)|^2$$

PG FROG is one of the most suitable FROG techniques to get single-shot measurement of ultrashort, multi TW laser systems, using a similar mechanism (time delay encoded in spatial position) to the one described above

R. Trebino *et al.*, Rev. Sci. Instr. **68**, 3277 (1997)

Second Harmonic Generation (SHG) FROG

For "low intensity" laser systems, 2nd harmonic generation ($\chi^{(2)}$) nonlinearity can be used instead

The setup is essentially the same as for noncollinear Intensity Autocorrelation, with spectral resolution added

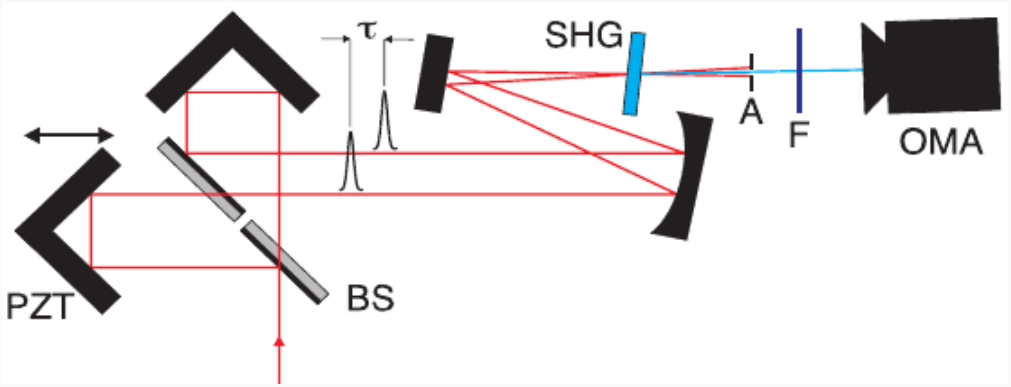

It is easy to check that in this case the gate is

$$g(t-\tau) = E(t-\tau)$$

and thus the signal

$$f_{signal}(t,\tau) = E(t)E(t-\tau)$$

Although very simple from the point of view of the experimental arrangement, SHG FROG provides rather unintuitive traces; this is due to the fact that the FROG trace depend, in general, on both the chirp of the pulse to be measured and the (possible) chirp of the gate pulse.

FROG reconstruction algorithm

The pulse field $E(t)$ can be completely retrieved by a FROG trace using an iterative algorithm (several variants exist). First notice that the knowledge of $E_{signal}(t,\tau)$ is enough to recover $E(t)$:

$$\int E_{signal}(t-\tau)\,\mathrm{d}\tau = \int E(t)E(t-\tau)\,\mathrm{d}\tau \propto E(t)$$

Writing $E_{signal}(t,\tau)$ as an Inverse Fourier Transform (with respect to τ) of a function

$$\tilde{E}_{signal}(t,\Omega) = \int_{-\infty}^{+\infty} \mathrm{d}\tau E_{signal}(t,\tau)\mathrm{e}^{-i\Omega\tau}$$

one easily realizes that the spectrogram is the (square) modulus of the 2D Fourier Transform of $E_{signal}(t,\Omega)$

$$S(\omega,\tau) = \left|\frac{1}{2\pi}\int \mathrm{d}t \int \mathrm{d}\Omega \tilde{E}_{signal}(t,\Omega)\mathrm{e}^{i\Omega\tau}\mathrm{e}^{-i\omega t}\right|^2$$

Unlike the 1D case, in 2D it is possible to recover a function knowing its (2D) spectrum

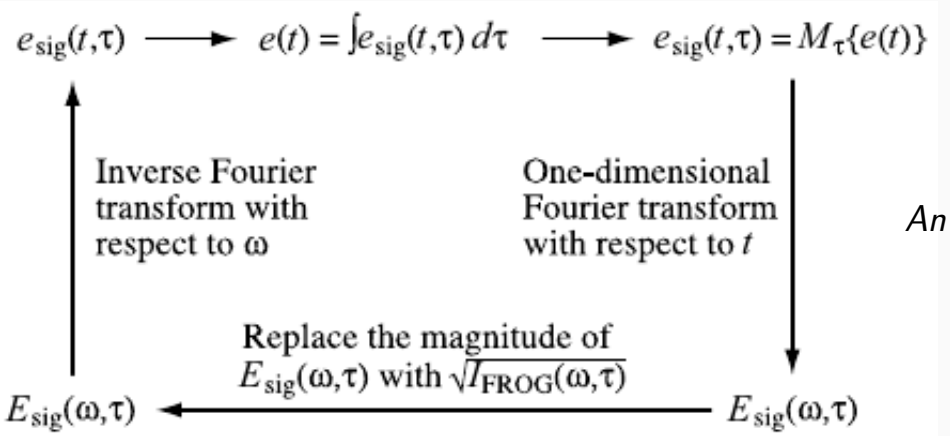

An example of an iterative FROG reconstruction algorithm

Examples of FROG traces

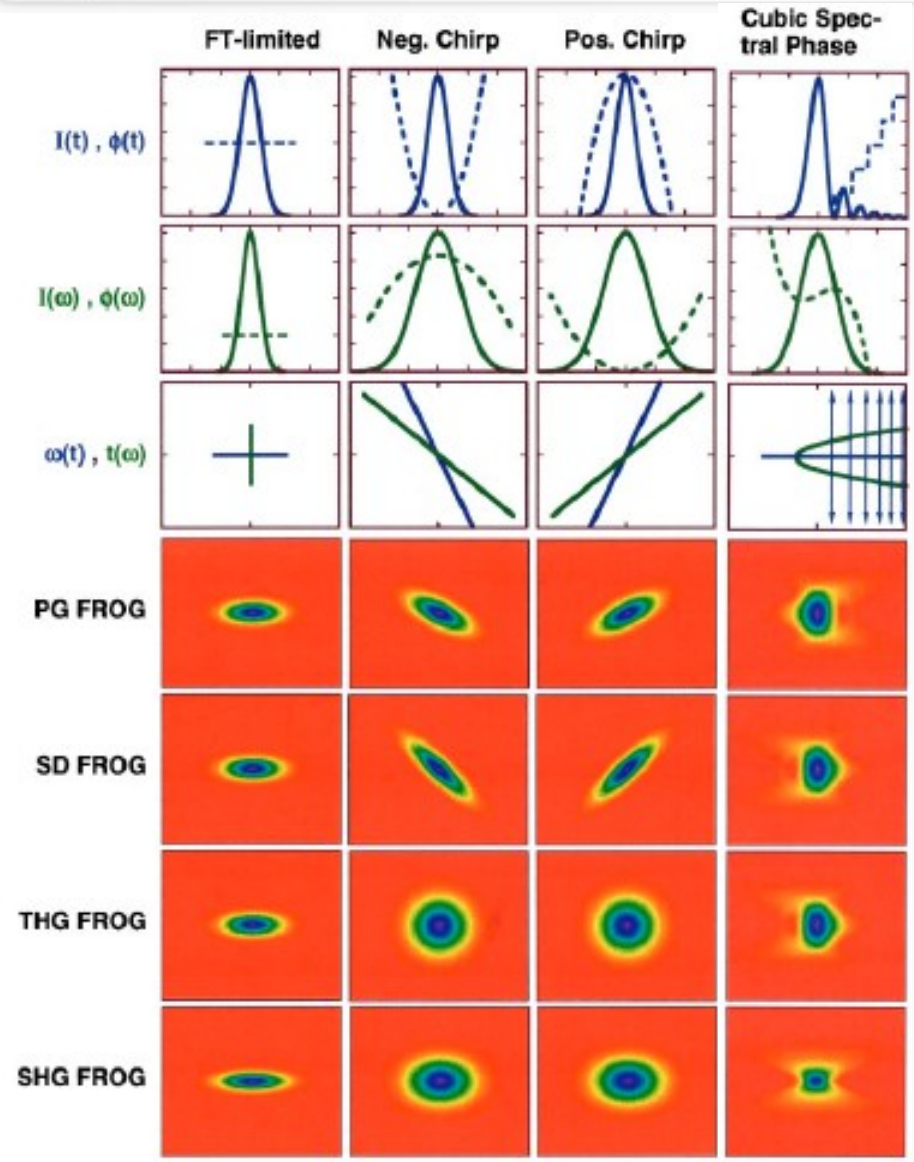

Few-cycles pulse

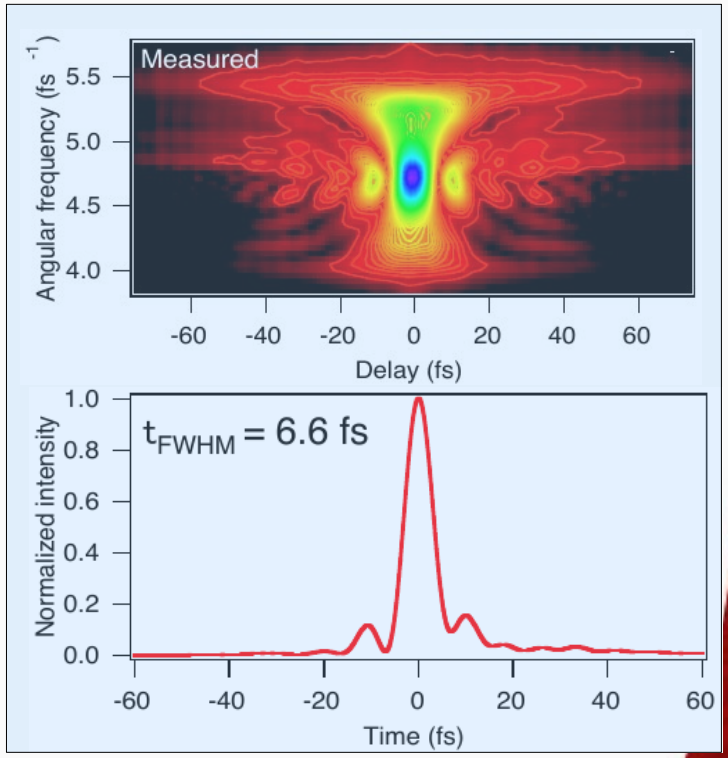

Spectral Phase Interferometry for Direct Electric Field Reconstruction

This can be considered an evolution of the Interferometric Autocorrelation: beside to be shifted in time, the two interfering pulses are also shifted in frequency (spectral shearing)

$$E_1(t) = A(t)\mathrm{e}^{i\omega_0 t}\mathrm{e}^{i\Phi_a(t)}$$
$$E_2(t) = A(t-\tau)\mathrm{e}^{i(\omega_0+\Omega)(t-\tau)}\mathrm{e}^{i\Phi_a(t-\tau)}$$

It is easy to verify that the measured spectrum is

$$\begin{aligned} S(\omega) &\propto \left|\mathcal{F}\left[E_1(t)+E_2(t)\right]\right|^2 \\ &= \left|\tilde{A}(\omega)\right|^2 + \left|\tilde{A}(\omega+\Omega)\right|^2 + 2\left|\tilde{A}(\omega)\right|\left|\tilde{A}(\omega+\Omega)\right|\cos\left[\omega\tau+\phi(\omega+\Omega)-\phi(\omega)\right] \end{aligned}$$

For a flat spectral phase, the overall power spectrum exhibits oscillations with period $2\pi/\tau$.
For chirped pulses, the fringe separation depends on the spectral phase difference

If the power spectrum is measured with sufficient resolution, this allows the determination of the spectral phase.

In this case, no iterative algorithm is needed (analysis only involves FT, filtering in the frequency domain, IFT, ...)

See Ch. Iaconis *et al.*, IEEE Journ. Quantum Electr. **35**, 501 (1999)

SPIDER basic setup

- Pulse split into two beams

- First arm: a replica of the pulse is generated (using for instance an etalon) with a given delay

- Second arm: the pulse passes through a stretcher, which broadens the pulse in time and give it a chirp (~quadratic spectral phase, linear chirp)

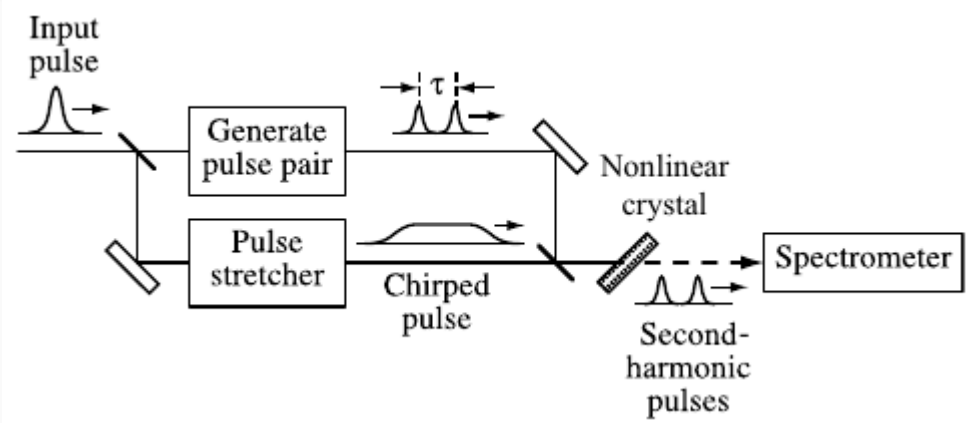

- The pulse pair (resulting from the first arm) and the stretched pulse then interact in a nonlinear crystal. The phase matching is set so as to only allow the SFG from a photon of each of the two replica and a photon of the stretched pulse.
Since the frequency of the stretched pulse at the time of interaction with each of the two replica is different, this actually corresponds to a spectral shear of the upconverted pulses with respect to each other

- Finally, the upconverted power spectrum is measured using a spectrometer

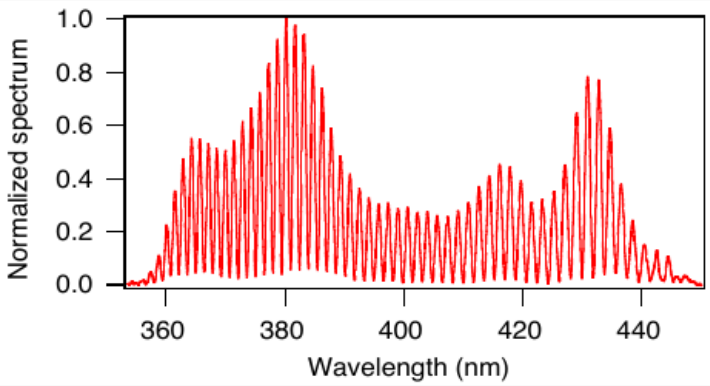

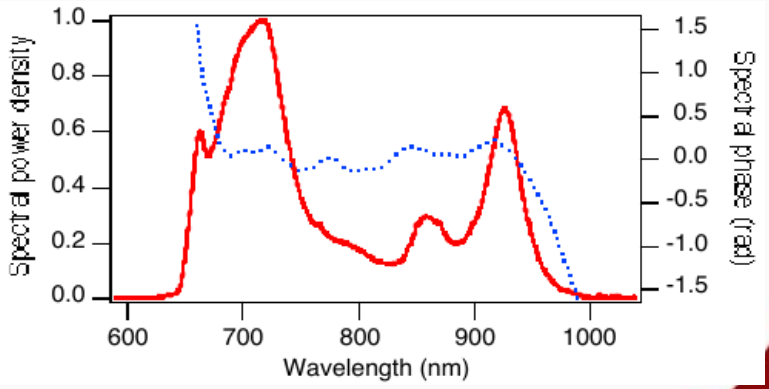

Pulse characterization methods: a comparison

To summarize on the pulse measurement techniques so far:

Autocorrelation

Non-collinear (or Intensity Autocorrelation): no phase information
Collinear: very limited phase informations

Frequency Resolved Optical Gating (FROG)

Gives amplitude and phase information
One setup may cover a large range of pulse durations
Based on iterative algorithms (not suitable for very high rep rate lasers)

Spectral Phase Interferometry for Direct Electric Field Reconstruction

Gives phase information
Straightforward to extend to significantly short pulse
Direct measurement of the spectral phase: no need of iterative algorithm (very fast)

Outline

Lecture 1 of 2

A (not so short) introduction to the mathematical description of the temporal behaviour of ultrashort laser pulses (terminology,, basic facts, ...)

- Spectral amplitude and phase
- Dispersion, dispersion compensation

Experimental techniques for the temporal characterization of ultrashort laser pulses

- Photodiodes, streak camera
- 1st and 2nd order autocorrelators

Lecture 2 of 2

- Advanced techniques for the pulse length and spectral phase measurements: FROG, SPIDER
- Contrast measurement techniques (in brief)

Transverse functions characterization and wavefront correction

- Wavefront characterization techniques
- Wavefront correction and beam focusing

Characterization of the transverse wavefront of a laser beam

Motivation (simple): ultrashort and ultraintense laser systems typically feature a large number of elements, whose optical performances can be greatly affected by material non-uniformity, manufacturing imperfections, material stresses, thermally induced deformations, ...
All these factors can introduce wavefront aberrations, which in turn affect the energy distribution in the focal plane

Furthermore, aberrations introduced by the focusing device (most often an Off-Aaxis Parabolic mirror) can be measured and possibly corrected using active (deformable) mirrors

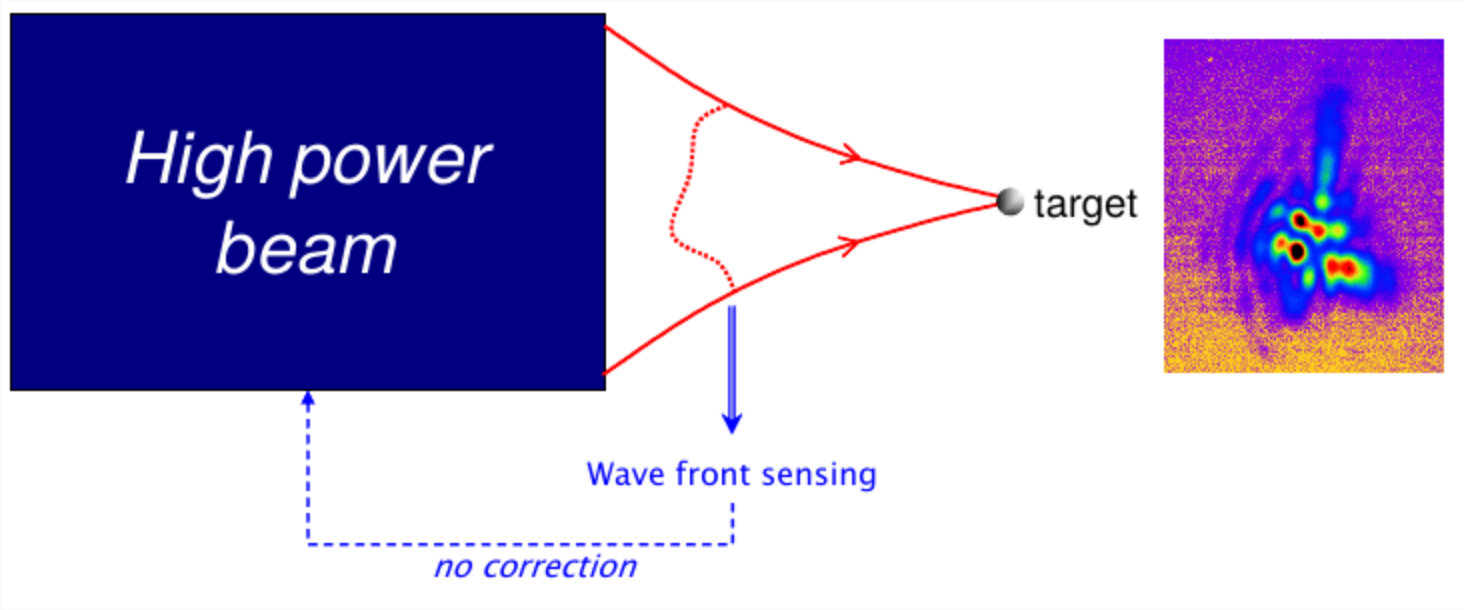

Main (low order) wavefront aberrations

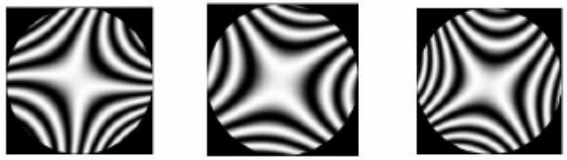

Astigmatism: Magnitude [0/1] , angle 0, 45°, 90

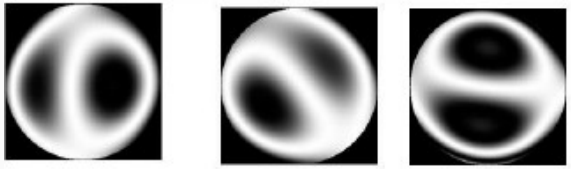

Coma: Magnitude [0/+1] 1, angle 0°, 45°, 90°

0.2 0.4 0.6 0.8 1

Spherical aberration [-1/+1]

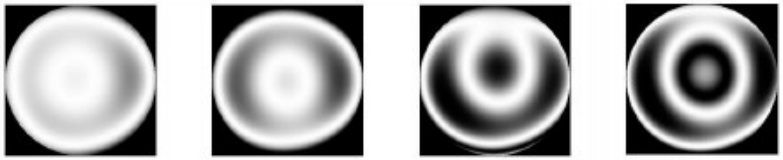

-0.2 -0.4 -0.6 -0.8

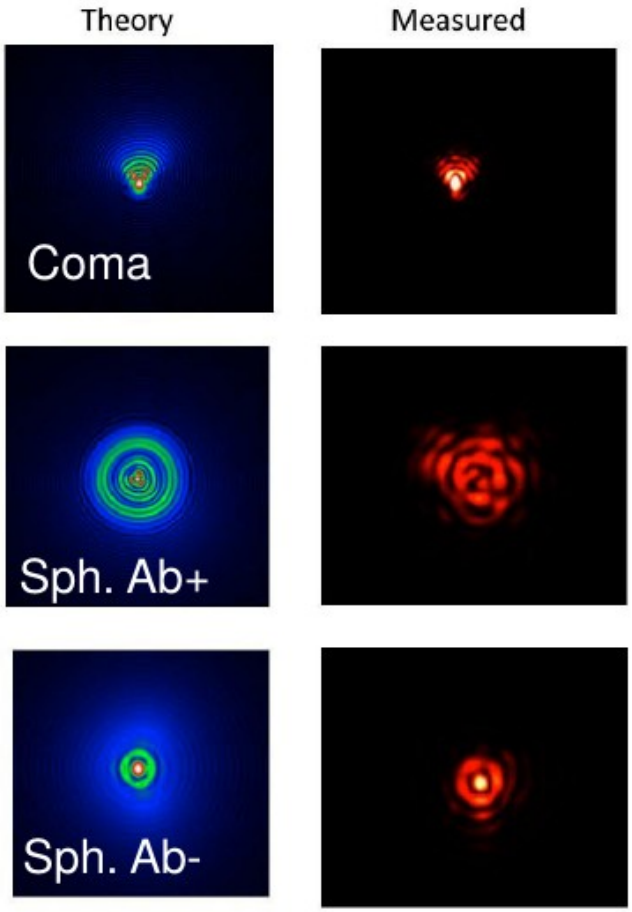

Characterization of the transverse wavefront of a laser beam

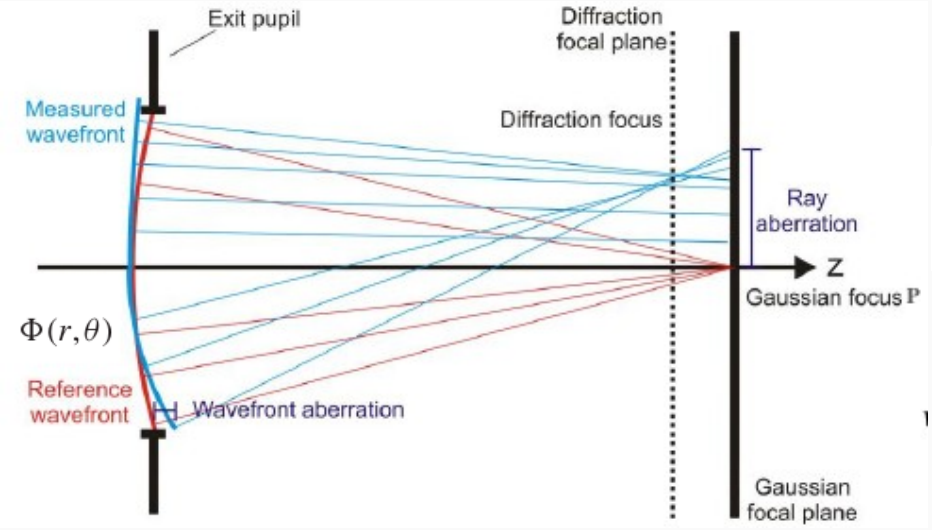

Most of the time the deviation of the wavefront from a plane is described in terms of Zernike polynomials, which forms a complete set of polynomials onto the unit circle:

$$\Phi(r,\theta) = A_{00} + \frac{1}{\sqrt{2}}\sum_{n=2}^{\infty} A_{n0} R_n^0(\rho) + \sum_{n=1}^{\infty}\sum_{m=1}^{n} A_{nm} R_n^m(\rho)\cos(m\theta)$$

with

$$Z_n^m(\rho,\theta) = R_n^m(\rho)\mathrm{e}^{\mathrm{i}m\theta}$$

$$R_n^m(\rho) = \frac{1}{2^k k!}\frac{1}{\rho^m}\left[\frac{1}{\rho}\frac{\mathrm{d}}{\mathrm{d}\rho}\right]^k\left[(\rho^2-1)^k \rho^{n+m}\right]$$

Strehl ratio: gives the maximum intensity achievable with an aberrated beam normalized to the one from an unaberrated one (see Born&Wolf for a deeper discussion)

$$i(P) = \frac{I(P)}{I^\star} = \frac{1}{\pi^2}\left|\int_0^1\int_0^{2\pi} \mathrm{e}^{\mathrm{i}[k\Phi(Y_1^\star,\rho,\theta) - v\rho\cos(\theta-\psi) - \frac{1}{2}u\rho^2]}\rho\,\mathrm{d}\rho\,\mathrm{d}\theta\right|^2.$$

The Strehl ratio is related to the mean square deformation of the wavefront:

$$\frac{I}{I_0} = 1 - k^2\left[\overline{\Phi^2} - (\overline{\Phi})^2\right]$$

The Strehl ratio can be written as a function of the coefficients of the expansion in terms of Zernike polynomials:

$$\frac{I}{I_0} = 1 - \frac{k^2}{2}\sum_{n=1}^{\infty}\sum_{m=0}^{\infty}\frac{A_{nm}^2}{n+1}$$

Wavefront Sensors (WFS) for (ultra)short laser pulses

For the characterization of (ultra)short laser pulses, two types of WFS are most often employed

Shack-Hartmann WFS

Measures the displacements (with respect to an unaberrated beam) of the spot of different beamlets focused by an array of lenses

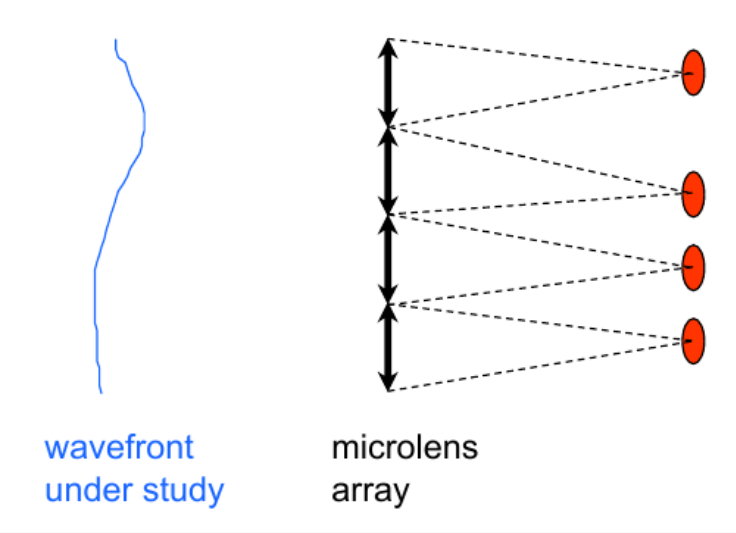

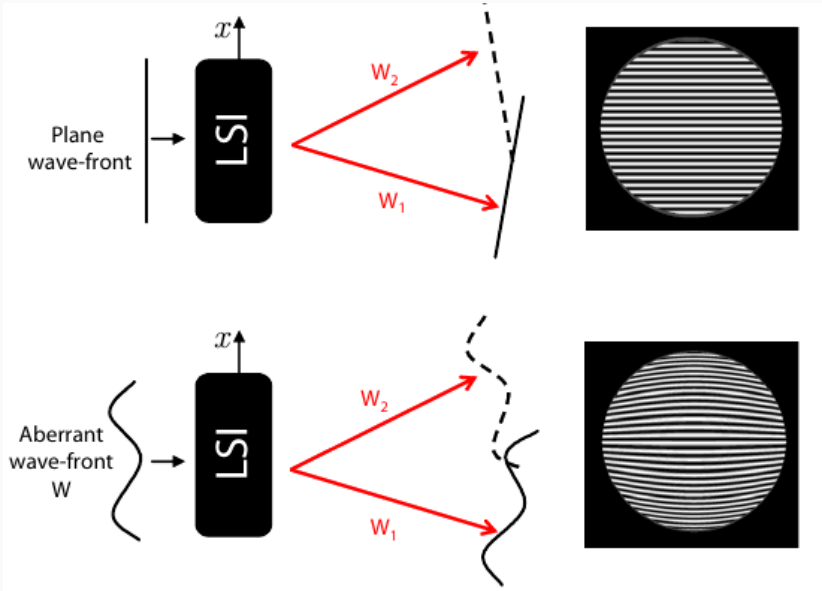

Lateral Shearing Interferometry

Measures the interference of 2 or more replicas of the impinging wavefront

For other WF measurement techniqes see H. Wang *et al.*, High Power Laser Sci. Tech. **2**, e25 (2014)

Shack-Hartmann WFS: the working principle

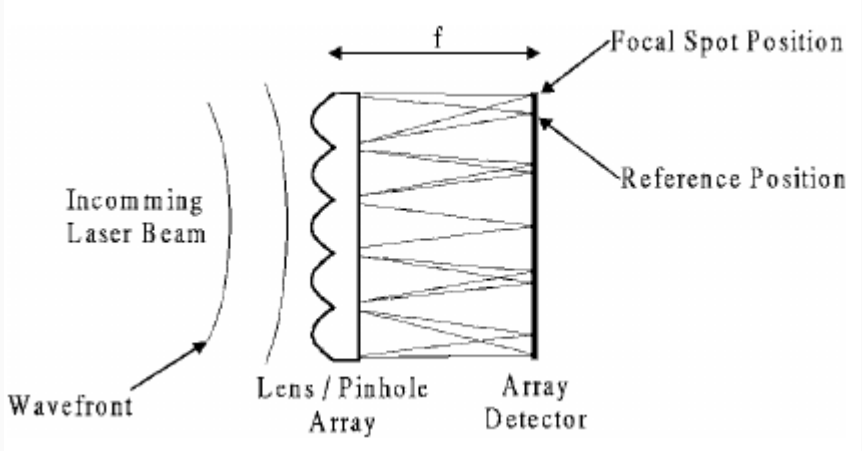

The spot deviation is related to the slope of the deformed wavefront

The displacements of the spot centroids with respect to a plane wave reference position is a measure of the local Poyinting vector and thus the local gradient of the wavefront

$$\hat{\mathbf{S}}_{\perp} = \begin{pmatrix} \partial w/\partial x \\ \partial w/\partial y \end{pmatrix}_{ij} = \boldsymbol{\beta}_{ij} = \frac{1}{f}\begin{pmatrix} x_c - x_r \\ y_c - y_r \end{pmatrix}_{ij}$$

These data can be used to reconstruct the wavefront, starting from a polynomial expansion (for instance, a Zernike expansion)

$$\beta_{ij}^{(x,y)} = \frac{\partial w(x,y)}{\partial (x,y)_{ij}} = \sum_{k=1}^{L} c_k \frac{\partial P_k(x,y)}{\partial (x,y)_{ij}}$$

Data from SH WFS can also be used to calculate "standard" beam parameters, such as the M^2 parameter:

$$M_x^2 = 2k\sqrt{\langle x^2\rangle \cdot \langle u^2\rangle - \langle xu\rangle^2}$$

which depends on 2nd order moments of the so-called Wigner distribution:

$$\langle x^2\rangle = \frac{\sum_{ij}(x_{ij} - \langle x\rangle)^2 I_{ij}}{\sum_{ij} I_{ij}} \qquad \langle xu\rangle = \frac{\sum_{ij}(\beta_{x,ij} - \langle \beta_x\rangle)\cdot(x_{ij} - \langle x\rangle)\cdot I_{ij}}{\sum_{ij} I_{ij}}$$

$$\langle u^2\rangle = \frac{\sum_{ij}(\beta_{x,ij} - \langle \beta_x\rangle)^2 I_{ij}}{\sum_{ij} I_{ij}} + \frac{1}{k^2}\frac{\sum_{ij}(1/I_{ij})(\partial I/\partial x)_{ij}^2}{4\sum_{ij} I_{ij}}$$

For a complete discussion of the analysis of SH WFS see B. Schafer *et al*, Rev. Sci. Instrum. **77**, 053103 (2006)

Using WFS in ultrashort laser systems in combination with deformable mirrors (DM)

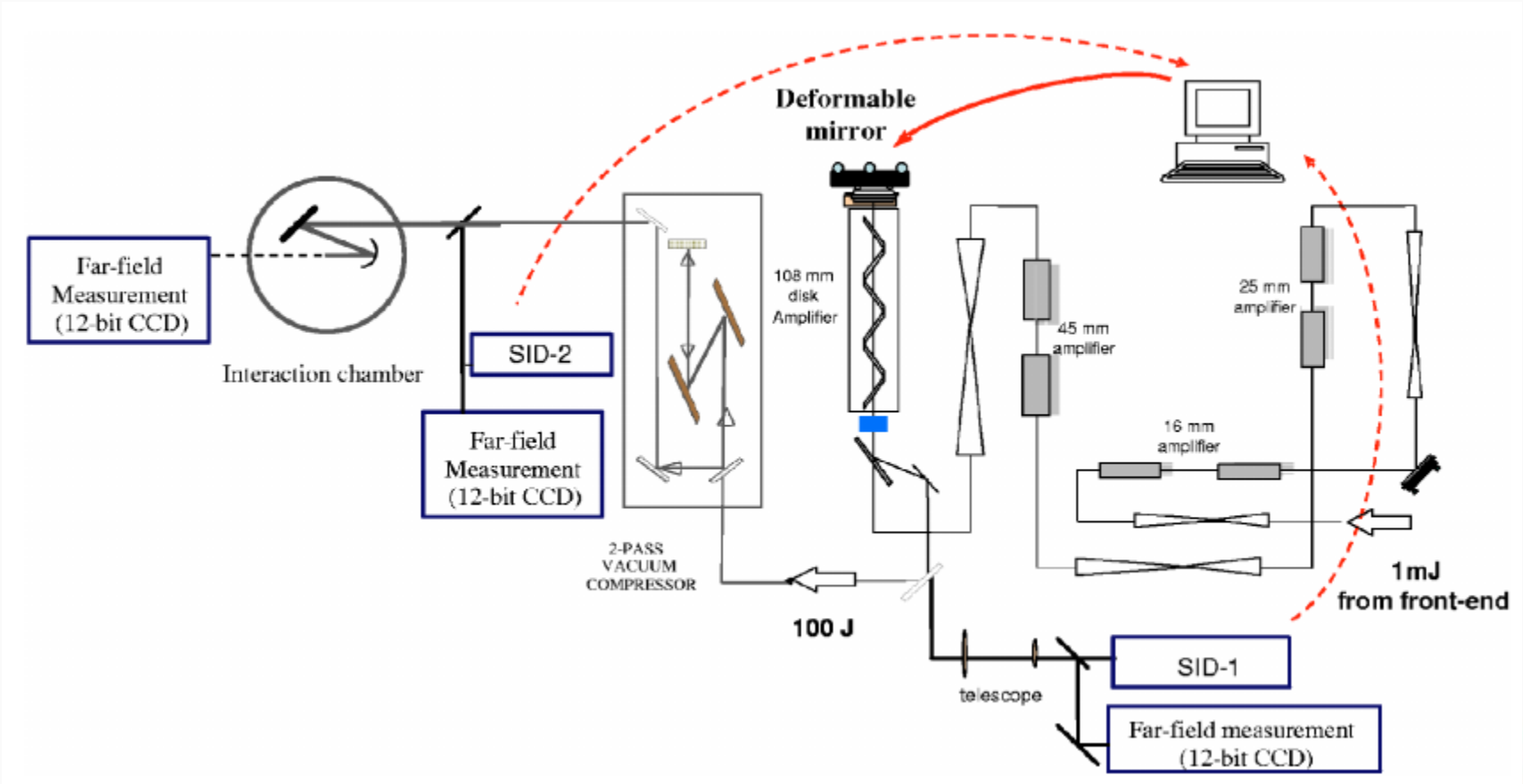

Wattellier *et al.*, Rev. Sci. Instrum. **75**, 5186 (2004)

An example of Shack-Hartmann WFS data

Raw image from SH detector

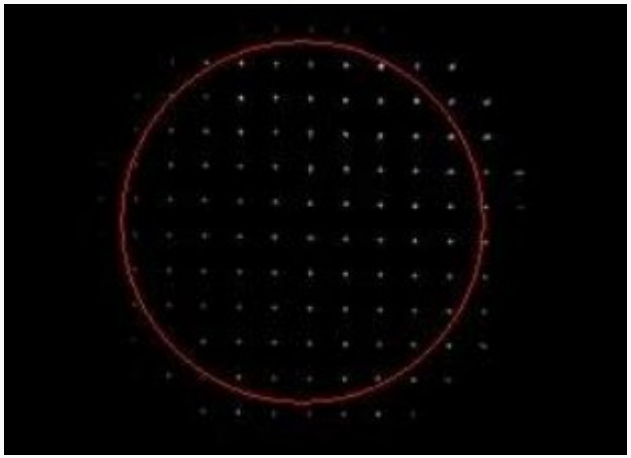

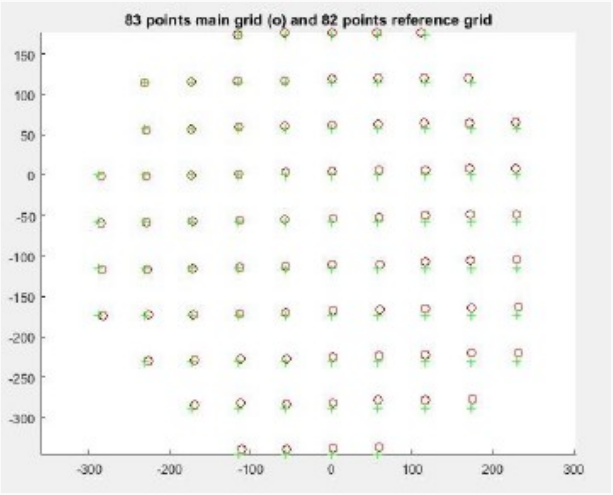

Calculated centroid positions

Retrieved local displacement from local reference centroid

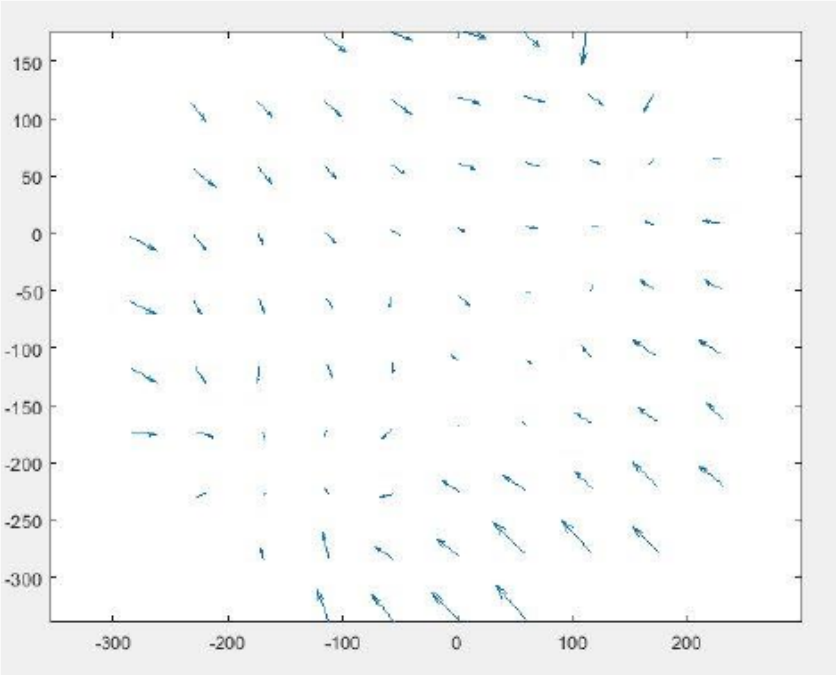

Data taken @ILIL-CNR Pisa

An example of Shack-Hartmann WFS data

Retrieved wavefront

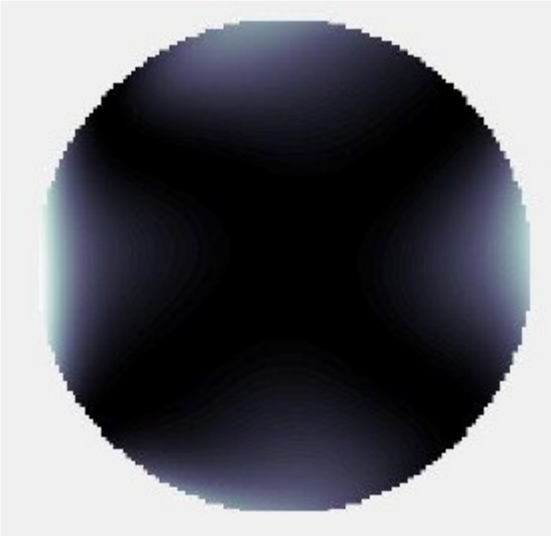

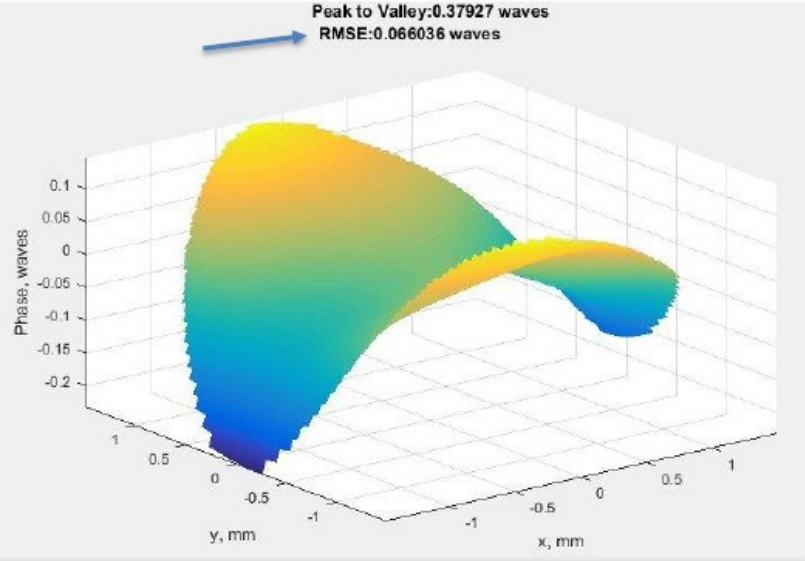

Retrieved coefficients of the Zernike expansion

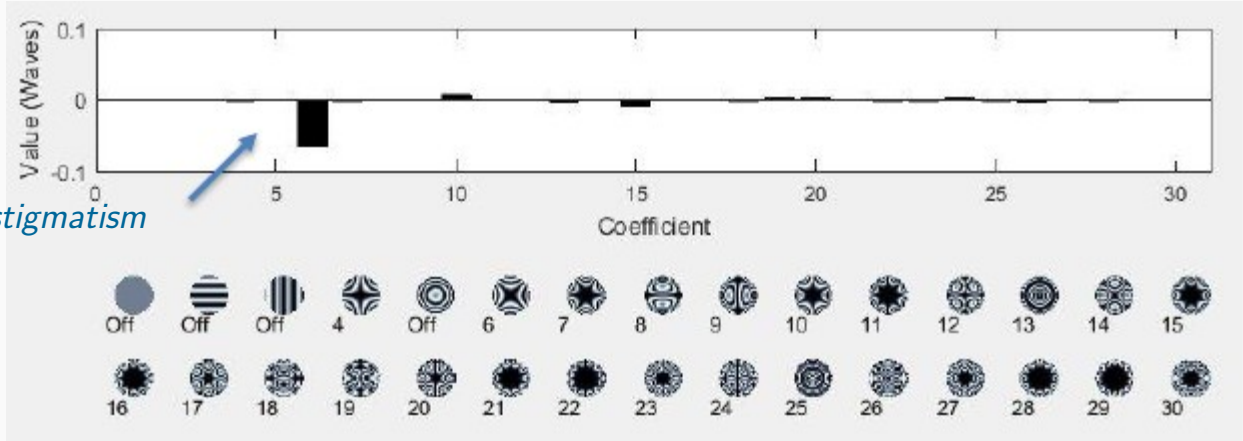

Vertical Astigmatism

Far-field distribution with and w/o active wavefront correction

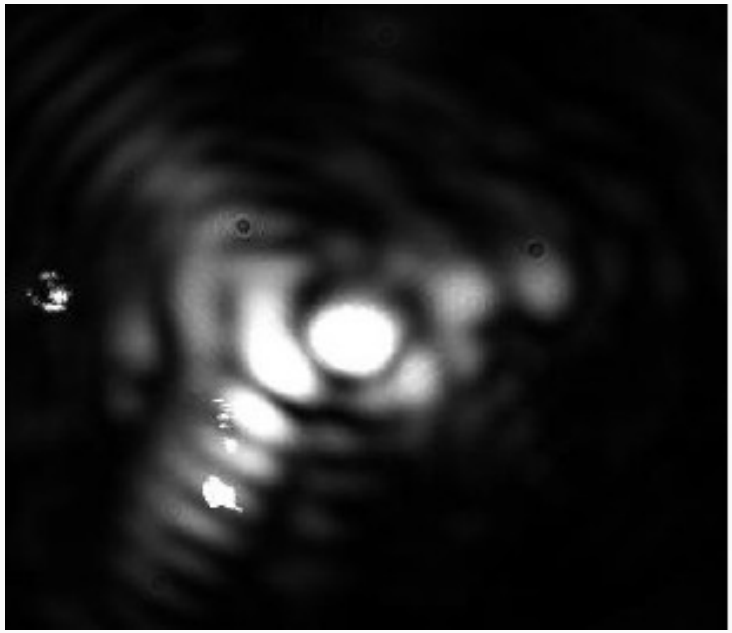

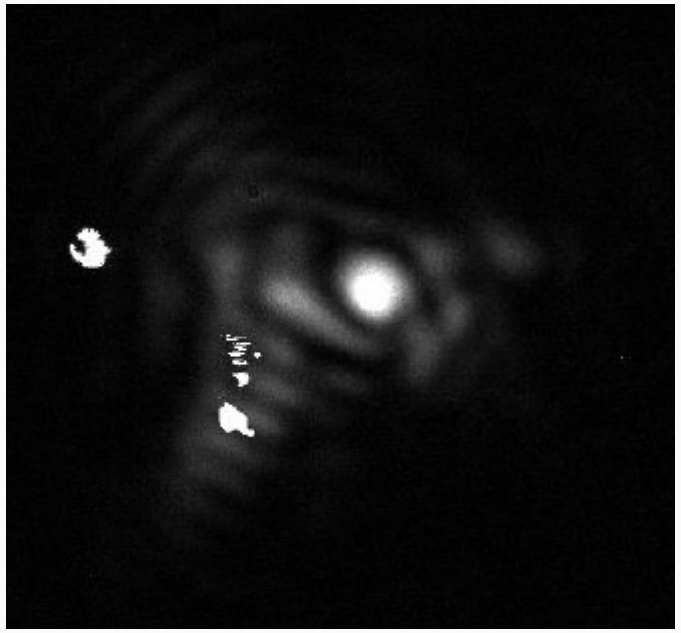

Data taken @ILIL-CNR Pisa

Wavefront correction from direct wavefront sensing in the far-field

Wavefront distortion leading can also be introduced by incorrect Off-Axis Parabola (focusing optics) alignment

Even for very small angles of misalignment, this results in focal spot broadening and thus both maximum intensity and Strehl ratio degradation

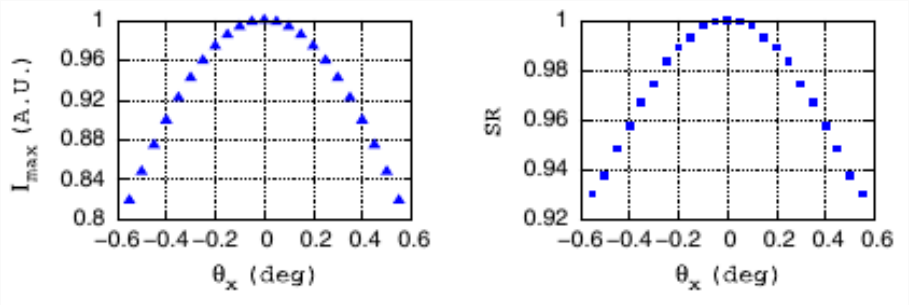

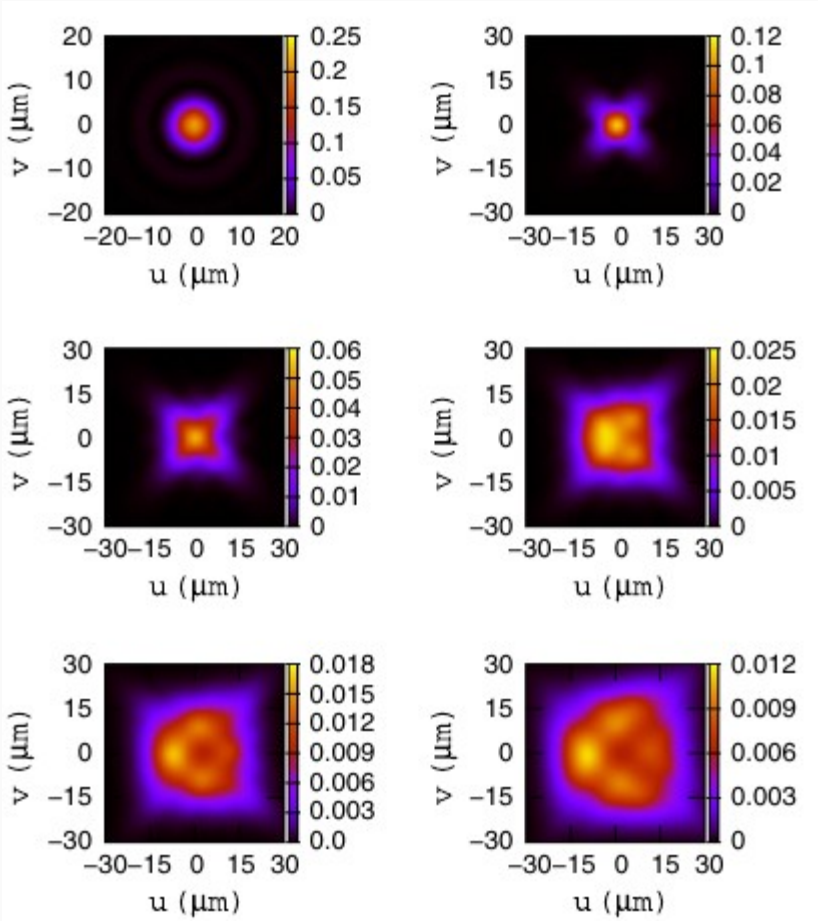

L. Labate *et al.*, Appl. Opt. **55**, 6506 (2016)

Wavefront correction from direct wavefront sensing in the far-field

Wavefront sensing and active correction with deformable mirrors can also be used to compensate for OAP misalignments

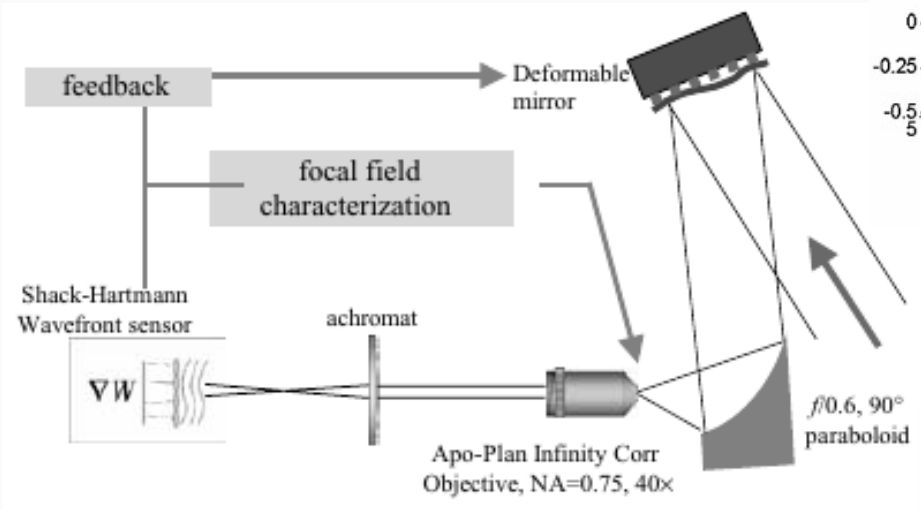

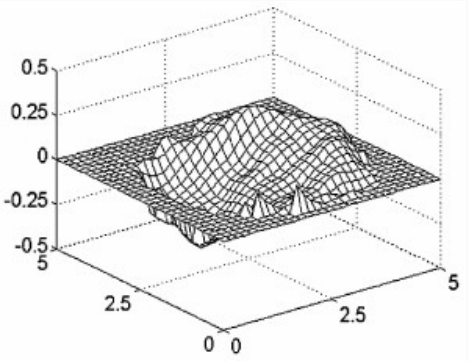

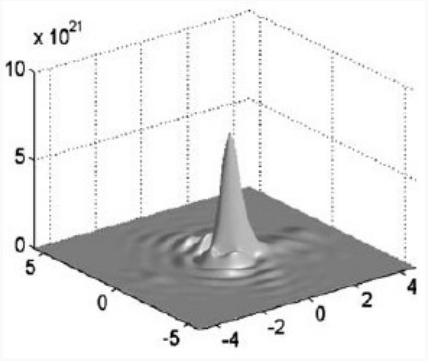

$I_{peak}=(6.9\pm0.7)\times10^{21}$ W/cm^2

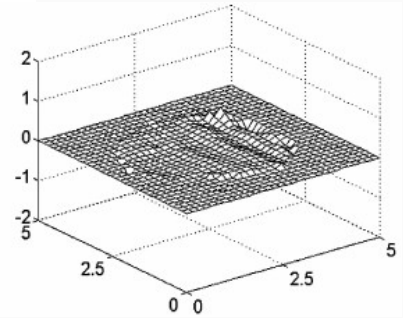

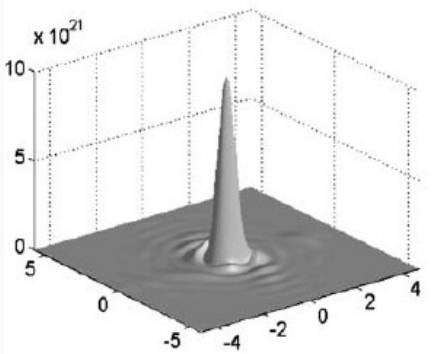

$I_{peak}=(1\pm0.1)\times10^{22}$ W/cm^2

Characterization of focal field formed by a large numerical aperture paraboloidal mirror and generation of ultra-high intensity (10^{22} W/cm^2)

S.-W. BAHK[1,*,✉]
P. ROUSSEAU[2]
T.A. PLANCHON[3]

Appl. Phys. B 80, 823–832 (2005)

Outline

Lecture 1 of 2

A (not so short) introduction to the mathematical description of the temporal behaviour of ultrashort laser pulses (terminology,, basic facts, ...)

- Spectral amplitude and phase
- Dispersion, dispersion compensation

Experimental techniques for the temporal characterization of ultrashort laser pulses

- Photodiodes, streak camera
- 1st and 2nd order autocorrelators

Lecture 2 of 2

- Advanced techniques for the pulse length and spectral phase measurements: FROG, SPIDER
- Contrast measurement techniques (in brief)

Transverse functions characterization and wavefront correction

- Wavefront characterization techniques
- Wavefront correction and beam focusing

Contrast measurement techniques

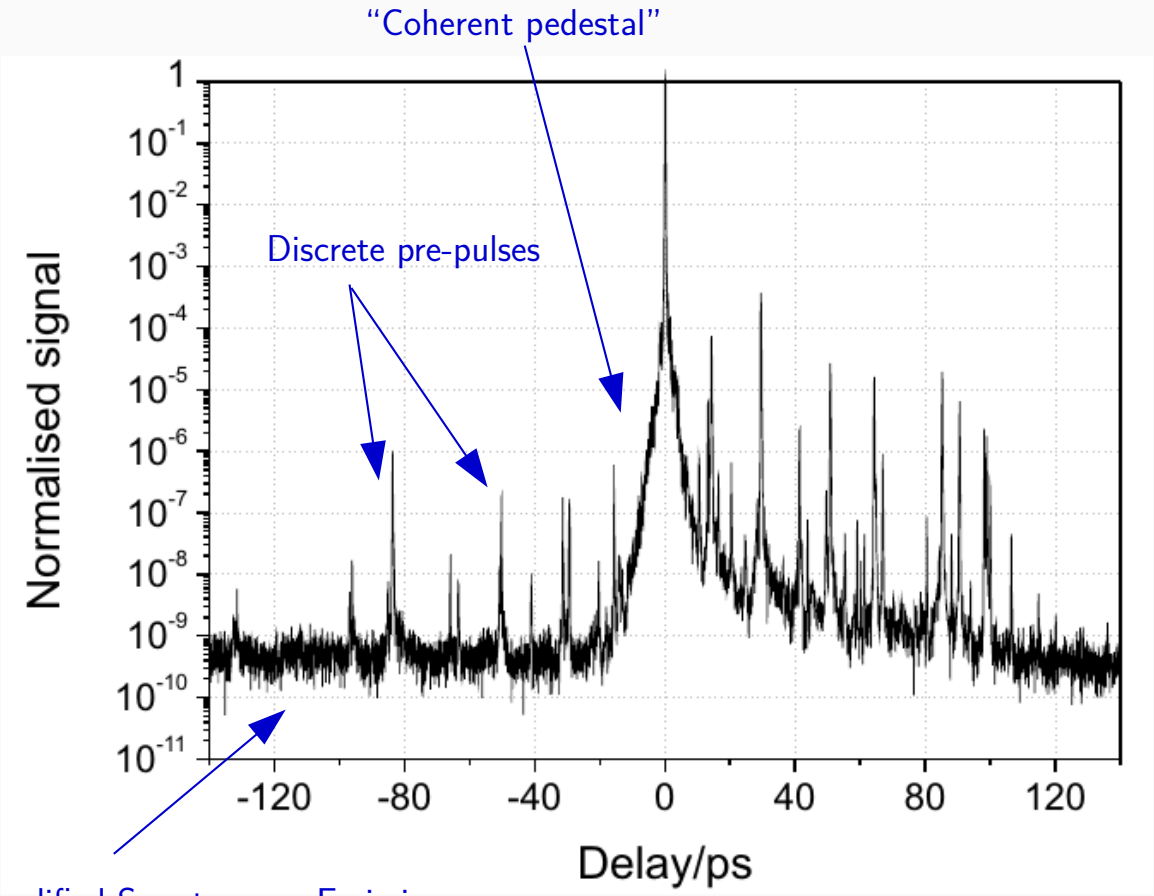

Remind: pulse contrast refers to the ratio of the peak intensity of a laser pulse (main peak) to its background

Different techniques have been developed to enhance the contrast (at all time ranges), such as the usage of cleaning Pockels cells, pre-amplification followed by the usage of saturable absorber, XPW, plasma mirrors, ...

Contrast measurement using 3rd order autocorrelation

Measuring the contrast of (modern) CPA laser systems requires high-dynamic range experimental methods and high S/N ratio

This can be achieved using a high order nonlinear process and also averaging over many samplings

Typical scheme for a contrast measurement technique based on 3rd order correlation

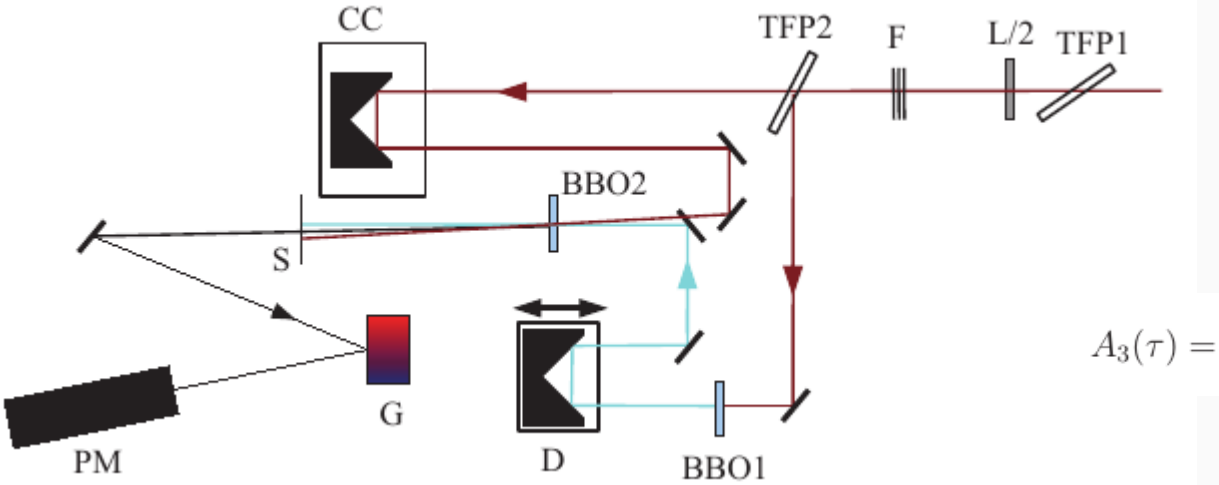

$$A_3(\tau) = \frac{\int I(t+\tau)I^2(t)dt}{\int I^3(t)dt}$$

This is essentially a repetitive (multi-shot) measurement (different times are sampled by a delay scanning)
Single-shot operation (although possible in principle) is hindered by the need of a) a high dynamic range and b) a large time span

Toward single-shot contrast measurement techniques

Single-shot contrast measurement technique based on the cross-correlation (via SFG) between tha pulse to be measured and a very clean "sampling" pulse, generated via OPG/OPA

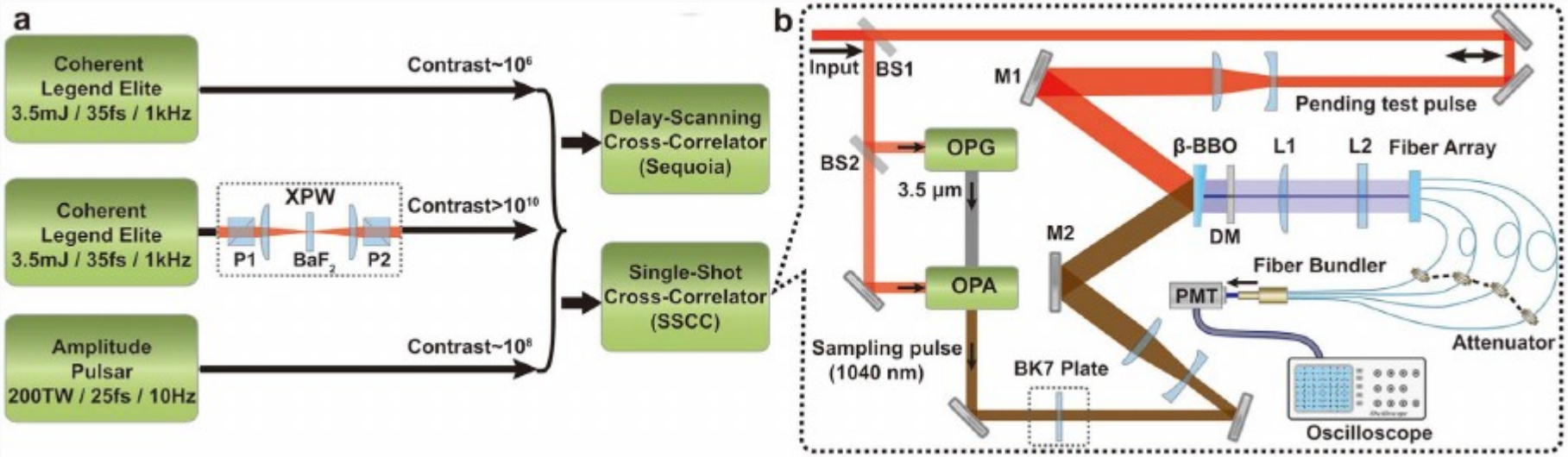

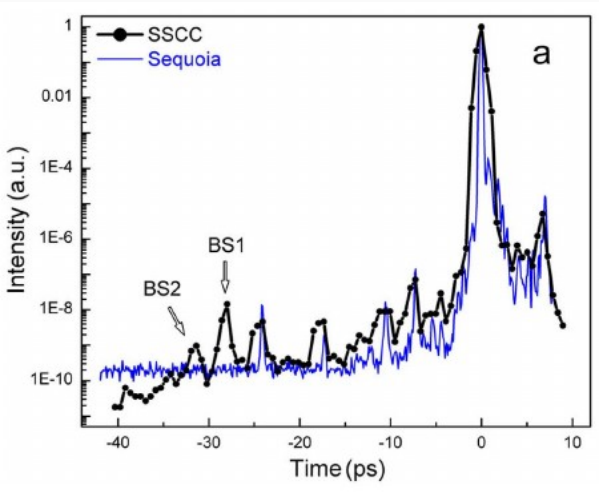

Single-shot measurement of $>10^{10}$ pulse contrast for ultra-high peak-power lasers

Yongzhi Wang[1], Jingui Mc

SCIENTIFIC REPORTS | 4 : 3818 | DOI: 10.1038/srep03818
Published
22 January 2014